



# LUND UNIVERSITY

## Core-polarization effects and radiative lifetime measurements in PrIII

Biemont, E; Garnir, H. P; Palmeri, P; Quinet, P; Li, Z. S; Zhang, Z. G; Svanberg, Sune

*Published in:*

Physical Review A (Atomic, Molecular and Optical Physics)

*DOI:*

[10.1103/PhysRevA.64.022503](https://doi.org/10.1103/PhysRevA.64.022503)

2001

[Link to publication](#)

*Citation for published version (APA):*

Biemont, E., Garnir, H. P., Palmeri, P., Quinet, P., Li, Z. S., Zhang, Z. G., & Svanberg, S. (2001). Core-polarization effects and radiative lifetime measurements in PrIII. *Physical Review A (Atomic, Molecular and Optical Physics)*, 64(2). <https://doi.org/10.1103/PhysRevA.64.022503>

*Total number of authors:*

7

### General rights

Unless other specific re-use rights are stated the following general rights apply:

Copyright and moral rights for the publications made accessible in the public portal are retained by the authors and/or other copyright owners and it is a condition of accessing publications that users recognise and abide by the legal requirements associated with these rights.

- Users may download and print one copy of any publication from the public portal for the purpose of private study or research.
- You may not further distribute the material or use it for any profit-making activity or commercial gain
- You may freely distribute the URL identifying the publication in the public portal

Read more about Creative commons licenses: <https://creativecommons.org/licenses/>

### Take down policy

If you believe that this document breaches copyright please contact us providing details, and we will remove access to the work immediately and investigate your claim.

LUND UNIVERSITY

PO Box 117  
221 00 Lund  
+46 46-222 00 00

## Core-polarization effects and radiative lifetime measurements in Pr III

E. Biémont,<sup>1,2</sup> H. P. Garnir,<sup>1</sup> P. Palmeri,<sup>2</sup> P. Quinet,<sup>2</sup> Z. S. Li,<sup>3</sup> Z. G. Zhang,<sup>3</sup> and S. Svanberg<sup>3</sup><sup>1</sup>*Institut de Physique Nucleaire, Atomique et de Spectroscopie, (Bâtiment B15), Université de Liège, Sart Tilman, B-4000 Liège, Belgium*<sup>2</sup>*Astrophysique et Spectroscopie, Université de Mons-Hainaut, B-7000 Mons, Belgium*<sup>3</sup>*Department of Physics, Lund Institute of Technology, P.O. Box 118, S-211 00 Lund, Sweden*

(Received 18 October 2000; published 10 July 2001)

New radiative lifetimes of eight levels in Pr III have been measured using the time-resolved laser-induced fluorescence method. A tunable frequency-doubled dye laser with 1-ns pulse duration was used to excite selectively doubly ionized praseodymium in a laser-produced plasma. The experimental results agree generally well with theoretical data, provided core-polarization effects are considered in the calculations in an adequate way.

DOI: 10.1103/PhysRevA.64.022503

PACS number(s): 32.70.Cs, 42.62.Fi

## I. INTRODUCTION

Pr III, which is suspected to be present or has been observed in different types of stars [1–4], is very important in astrophysics. An accurate and reliable knowledge of the praseodymium content in chemically peculiar stars is indeed needed to complete our knowledge of the abundance systematics, and to deduce, for these stars, a successful theory of fractionation accounting for the available observations.

Atomic transition probabilities are a key parameter for a determination of the chemical composition of the stars. Available radiative data for the third spectrum of the rare-earth elements are generally very fragmentary. This is related to the complexity of the atomic configurations involved with an unfilled  $4f$  shell, which renders accurate calculations extremely difficult (relativity and correlation have to be considered simultaneously and in a detailed way) and also to the difficulty to produce experimentally these doubly ionized ions. With the increasing resolution and high signal-to-noise spectra now available for many stars (see, e.g., Refs. [5], [6]), it is increasingly important to obtain more information about the radiative parameters for the rare-earth atoms and ions in general and for Pr III more specifically.

The first set of transition probabilities for Pr III was obtained very recently by Palmeri *et al.* [7]. A Hartree–Fock method with relativistic corrections (HFR approach), combined with a least-squares fitting of the available experimental levels, including a number of newly determined values, was used for the calculation of eigenfunctions and eigenvalues. Extensive configuration interaction and core-polarization effects were introduced in the calculations. The new  $f$  values were used to determine the chemical composition of the stars HD 101065 (Przybylski’s star) and HD 141556 ( $\chi$  Lupi).

However, recent detailed comparisons between HFR theoretical data and experimental lifetimes in Er III [8] and Tm III [9] showed that theoretical oscillator strengths of the  $4f$ - $5d$  transitions may be affected by large uncertainties. This results from the fact that the analytical core-polarization corrections to the dipole operator as used in Ref. [7] are no longer valid for  $4f$ - $5d$  transitions. A correction procedure, consisting in applying a scaling factor to the uncorrected  $\langle 4f|r|5d \rangle$  radial matrix element, was successfully tested in

the cases of Er III [8], Tm III [9], Ce II [10], and Yb IV [11]. It is one of the purposes of the present paper to verify the adequateness of this correction in the case of Pr III.

In order to provide reliable experimental  $f$  values and to check the previous theoretical results [7], lifetime measurements in Pr III, performed with an accurate laser technique, are most welcome. In the present paper, values for levels involving excitation in the range between 58 000 and 65 000  $\text{cm}^{-1}$  were carried out at the vacuum ultraviolet (VUV) laboratory of the Lund Laser Center [12], and are described in the following sections. The new lifetimes are used in combination with theoretical branching ratios, in order to deduce a new set of oscillator strengths in Pr III.

## II. MEASUREMENTS AND RESULTS

The ground electronic configuration of the  $\text{Pr}^{2+}$  ion is  $4f^3$ . Through a two-step excitation from the ground state  $4f^3 \ ^4I_{9/2}^o$ , radiative lifetimes of three excited states of the  $4f^2 5d^2$  configuration and five excited states of the  $4f^2 6p$  configuration were measured using time-resolved laser-induced fluorescence.

The Pr III levels, compiled at National Institute for Standards and Technology (NIST) [13], were taken from Sugar’s analysis [14,15] with some additions and revisions made in

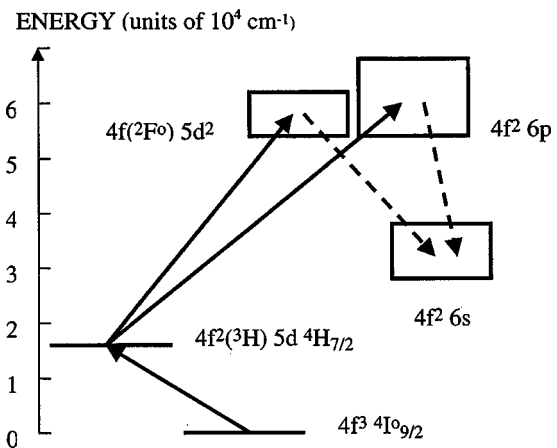


FIG. 1. Partial Grotrian diagram for Pr III, with transitions involved in the present work.

TABLE I. Pr III levels measured, and excitation schemes.

Levels <sup>a</sup>	Energy (cm <sup>-1</sup> )	Excitation $\lambda_{\text{air}}$ (nm)	Laser mode <sup>b</sup>	Observed $\lambda_{\text{air}}$ (nm)
$4f^2(^4H_4)6p_{1/2} J=\frac{7}{2}$	58158.1	237.90	2w + SS	335.94
$4f^2(^4H_4)6p_{1/2} J=\frac{9}{2}$	58174.1	237.81	2w + SS	335.76
$4f^2(^4H_4)6p_{3/2} J=\frac{7}{2}$	61605.7	219.70	2w	301.06
$4f(^2F)5d^2(^3F) J=\frac{9}{2}$	62535.6	215.22	2w	314.35
$4f^2(^3F_2)6p_{1/2} J=\frac{5}{2}$	63576.3	210.72	2w	330.62
$4f(^2F)5d^2(^3F) J=\frac{9}{2}$	64235.6	207.83	2w	300.74
$4f^2(^3F_3)6p_{1/2} J=\frac{5}{2}$	64401.0	207.13	2w	338.02
$4f(^2F)5d^2(^3F) J=\frac{5}{2}$	64817.5	205.35	2w	333.33

<sup>a</sup>From Ref. [13].

<sup>b</sup>2w means the frequency doubled in a KDP crystal and, eventually, Raman shifted (SS indicates the second Stokes component) in hydrogen gas.

Refs. [16–18]. More recently, a new analysis of the Pr III energy-level scheme was realized by Wyart and Palmeri [19]. A partial energy-level scheme relevant to the present experiment is shown in Fig. 1, and the excitation transitions and detected fluorescence decay channels are indicated as well. More details on the excitation for each individual level are shown in Table I. For the first step, from the ground state, a 619.56-nm laser was utilized to excite the  $5d\ ^4H_{7/2}$  state, which has a lifetime longer than 200 ns [7]. From this level, in a second step, the selected upper levels of the  $4f^26p$  and  $4f5d^2$  configurations were populated by a further short-duration-pulse tunable UV laser.

The experimental setup used in the present experiment is shown in Fig. 2. Two dye lasers (Continuum ND-60), which operated on the 4-dicyanomethylene-2-methyl-6-p-dimethylaminostyryl-4H-pyran (DCM) dye, were pumped separately by two neodymium-doped yttrium aluminum garnet (Nd:YAG) lasers (Continuum NY-82) (lasers *B* and *C* in Fig. 2). One of the two dye lasers was tuned to 619.56 nm in order to be used in the first step to excite the  $4f^2(^3H) 5d\ ^4H_{7/2}$  state at  $16\,135.97\text{ cm}^{-1}$ . Before being sent to pump the second dye laser, the output from the second Nd:YAG laser

(laser *C* in Fig. 2) is shortened by a stimulated Brillouin scattering pulse compressor to about 1 ns (see technical details in Ref. [20]). The output laser pulses from the dye laser, which had a pulse duration of about 1.5 ns, were frequency doubled in a potassium dihydrogen phosphate (KDP) crystal (2w), and sometimes further Raman shifted (2w + 1S, 1S indicating the first Stokes component) in hydrogen gas, to provide the tunable UV radiation for reaching the selected upper levels of the second step. Another small Nd:YAG laser (Continuum Surelite) (laser *A* in Fig. 2), which provided 10-ns pulses of about 5-mJ energy at 532 nm, was employed to perform the ablation on a praseodymium target. All three Nd:YAG lasers were working in an external triggering mode, and were triggered by two mutual connected Stanford Research Systems Model 535 digital delay generators. This enables the temporal synchronization of the two laser pulses for the first and second step excitations, and also a free variation of the delay time between the atomization and excitation laser pulses. The ablation laser pulses were sent from the top of the vacuum system through a glass window, and were focused on a rotating metallic praseodymium target. A short interval after the impinging of the pulse, the expanding

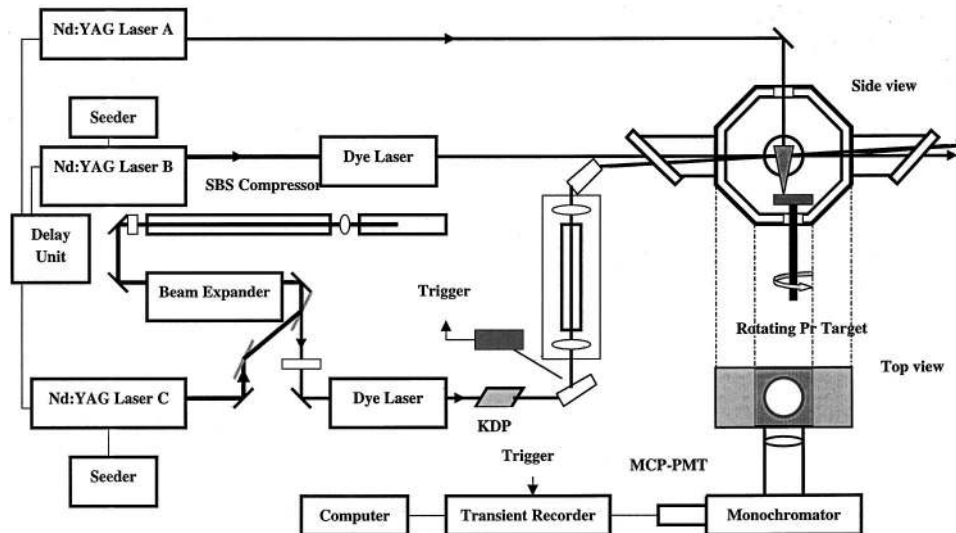


FIG. 2. Schematic drawing showing the experimental setup used in this work.

TABLE II. Experimental lifetimes and comparison with theoretical (HFR) results.

Energy <sup>a</sup> (cm <sup>-1</sup> )	<i>J</i>	Lifetime (ns)		
		Experiment	Theory This work <sup>b</sup>	Ref. [7]
58158.1	$\frac{7}{2}$	2.12(20)	2.06	2.25
58174.1	$\frac{7}{2}$	1.81(20)	1.71	1.95
61605.7	$\frac{7}{2}$	1.51(20)	1.75	1.97
62535.6	$\frac{7}{2}$	12(1)	8.23	26.99
63576.3	$\frac{7}{2}$	1.72(20)	1.68	1.91
64235.6	$\frac{7}{2}$	3.88(30)	3.37	5.17
64401.0	$\frac{7}{2}$	2.50(20)	2.85	3.35
64817.5	$\frac{7}{2}$	4.42(30)	3.45	5.12

<sup>a</sup>From Ref. [13].

<sup>b</sup>HFR calculation with empirical correction for  $4f$ - $5d$  transitions (see the text).

plasma was cooled down, with some of the doubly ionized praseodymium ions remaining in the cold plasma. The excitation beams were sent horizontally through this plasma about 1 cm above the target surface. As the lasers were tuned to the resonance frequencies, the designated upper levels were populated through a two-step excitation. Fluorescence photons in the spontaneous decay from the excited levels were recorded by a detection system, which included a 5-in. fused-silica lens, a  $\frac{1}{8}$ -m monochromator (resolution 6.4 nm/mm), and a Hamamatsu 1564U microchannel-plate (MCP) photomultiplier (200-ps rise time). The transient signals from the MCP were captured by a Tektronix TDS 684B digital oscilloscope 1-GHz bandwidth and a 5-GHz real-time sampling rate) and transferred to an IBM PC, where an online lifetime analysis was performed. The oscilloscope was triggered from a Thorlabs SV2-FC photodiode (120-ps rise time) driven by the excitation beam. The temporal shape of the excitation laser pulse was recorded with the fluorescence detection system by inserting a metal rod into the excitation beam, generating a scattering of the excitation laser radiation into the monochromator. The lifetimes were evaluated by fitting the recorded fluorescence signal with a convolution between the recorded laser pulse and a pure exponential decay (see details in Ref. [21]). Measurements under different conditions were performed to avoid systematic errors.

About 10–20 curves were recorded for each level, and the mean lifetime values were taken as the final results. The quoted error bars reflect not only the random scattering of different measurements, but also a conservative estimate of the possible remaining systematic errors. The results are shown in Table II, where a comparison with the theoretical calculations is presented.

### III. THEORETICAL CALCULATIONS

The  $\text{Pr}^{2+}$  ion is a La-like ion and, consequently has three valence electrons surrounding a Xe-like core. As a consequence, intravalence and core-valence interactions should both be taken into account for calculating the atomic structure. In practice, computer capabilities impose severe limita-

tions on the number of interacting configurations which can be considered simultaneously in the model. An approach in which most of the intravalence correlation is represented within a configuration-interaction (CI) scheme, while core-valence correlation is described by a core-polarization model potential with a core-penetration corrective term [22], was used by Palmeri *et al.* [7], who introduced the relevant corrections in the HFR equations [23]. CI was considered among the configurations:

$$\begin{aligned}
 &4f^3 + 4f^2np(n=6,7) + 4fnd^2(n=5,6) + 4fns^2(n=6,7) \\
 &\quad + 4f5dns(n=6,7) + 4f5dnd(n=6,7) \\
 &\quad + 4f^2nf(n=5,6) + 4f6p^2 + 4f6p7p \\
 &\quad + 5d6s6p + 4f6s7s + 5d^26p + 6s^26p + 6p^3
 \end{aligned}$$

for the odd-parity configurations, and

$$\begin{aligned}
 &4f^2nd(n=5,6,7) + 4f^2ns(n=6,7,8) + 4f5dnp(n=6,7) \\
 &\quad + 4f^25g + 4f5d5f + 4f6snp(n=6,7) + 5d^3 \\
 &\quad + 5d^26s + 5d^26d + 5d6s^2 + 5d6p^2 + 6s6p^2
 \end{aligned}$$

for the even-parity configurations. To compute the atomic orbitals and the radial integrals ( $E_{av}$ ,  $\zeta$ ,  $F^k$ ,  $G^k$ , and  $R^k$ ), the value of  $\alpha_d$ , the dipole polarizability, for the  $\text{Pr}^{5+}$  ion was chosen equal to  $5.40a_0^3$  [24]. For the cutoff radius  $r_c$ , a value

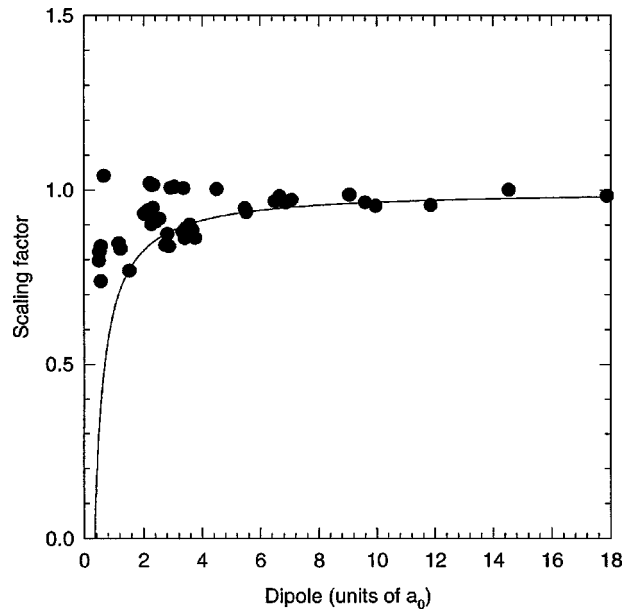


FIG. 3. Absolute value of the ratio between transition matrix elements corrected by core-polarization effects ( $d_{poi}$ ) and uncorrected matrix elements ( $d_{npoi}$ ) of transitions not involving a  $4f$  electron as a function of the absolute value of the uncorrected data. The filled circles appearing in the figure correspond to the 57 transition arrays generated by the configurations listed in the text. They are of the types  $4f^2nl$ - $4f^2n'l'$ ,  $4fnln'l'$ - $4fnln''l''$ , and  $nln'l'n''l''$ - $n'l'n''l''n'''l'''$ , where  $nl$ ,  $n'l'$ ,  $n''l''$ , and  $n'''l'''$  are different from the  $4f$  orbital.

TABLE III. Normalized oscillator strengths and transition probabilities for the intense ( $gf > 0.5$ ) lines depopulating the levels for which lifetimes have been measured.

Upper level <sup>a</sup>		Lower level <sup>a</sup>		$\lambda^b(\text{\AA})$	$\log gf$	$gA (s^{-1})$		
58158	( <i>o</i> )	3.5	16136	( <i>e</i> )	3.5	2378.974	-0.19	8.06E+08
58158	( <i>o</i> )	3.5	28399	( <i>e</i> )	3.5	3359.402	0.05	6.84E+08
58158	( <i>o</i> )	3.5	28885	( <i>e</i> )	4.5	3415.145	-0.15	4.31E+08
58174	( <i>o</i> )	4.5	12847	( <i>e</i> )	4.5	2205.479	-0.13	1.12E+09
58174	( <i>o</i> )	4.5	13352	( <i>e</i> )	5.5	2230.351	0.14	2.00E+09
58174	( <i>o</i> )	4.5	28399	( <i>e</i> )	3.5	3357.589	0.17	9.45E+08
58174	( <i>o</i> )	4.5	28721	( <i>e</i> )	4.5	3394.215	-0.30	3.13E+08
58174	( <i>o</i> )	4.5	28885	( <i>e</i> )	4.5	3413.271	-0.02	6.01E+08
61606	( <i>o</i> )	3.5	16516	( <i>e</i> )	3.5	2217.120	-0.14	8.04E+08
61606	( <i>o</i> )	3.5	28399	( <i>e</i> )	3.5	3010.606	0.32	1.26E+09
61606	( <i>o</i> )	3.5	28885	( <i>e</i> )	4.5	3055.298	-0.06	5.13E+08
63576	( <i>o</i> )	2.5	18990	( <i>e</i> )	3.5	2242.151	-0.25	7.64E+08
63576	( <i>o</i> )	2.5	33338	( <i>e</i> )	1.5	3306.156	-0.07	5.33E+08
63576	( <i>o</i> )	2.5	33660	( <i>e</i> )	2.5	3341.701	-0.23	3.59E+08
64236	( <i>o</i> )	4.5	30995	( <i>e</i> )	4.5	3007.451	-0.37	3.78E+08
64401	( <i>o</i> )	2.5	34825	( <i>e</i> )	3.5	3380.202	0.01	5.13E+08

<sup>a</sup>From Ref. [13]. (*o*) and (*e*) stand for odd and even, respectively.

<sup>b</sup>Calculated in air from the levels given in Ref. [13].

of  $1.67a_0$  was adopted. This value corresponds to the HFR average value  $\langle r \rangle$  for the outermost core orbitals ( $5p^6$ ) of the investigated valence configurations. Using a least-squares fitting procedure, the effective interaction parameters ( $\alpha$ ,  $\beta$ ,  $\gamma$ ) and the  $k$ -forbidden  $F^k$  and  $G^k$  integrals were adjusted to obtain the best agreement between the calculated eigenvalues and the observed energy levels taken from Refs. [13] and [19].

In the present calculation, the theoretical HFR method, as described by Palmeri *et al.* [7], was adopted with the same set of configurations and also the same values for the polarizability and cutoff radius. However, the procedure was modified in the following way. Detailed comparisons between theory and experiment in Er III [8] and Tm III [9] showed that  $4f$ - $5d$  transitions deserve special attention when considering atomic structure calculations in lanthanides in relation with the fact that  $4f$  electrons are deeply imbedded inside the Xe core. An attempt to solve the problem, originating from the fact that the analytical core-polarization corrections to the dipole operator as previously used are no more valid, consists of applying a scaling factor to the uncorrected  $\langle 4f|r|5d \rangle$  radial matrix element. This factor can be deduced from a curve showing the ratio between core-polarization corrected ( $d_{\text{pol}}$ ) and uncorrected ( $d_{\text{nopol}}$ ) transition matrix elements for transitions not involving a  $4f$  electron as a function of the uncorrected matrix element. In fact, the smooth curve derived by plotting  $|d_{\text{nopol}} - \Delta|/|d_{\text{nopol}}|$ , where  $\Delta = |d_{\text{nopol}} - d_{\text{pol}}|$  for transitions not involving a  $4f$  electron, is illustrated in Fig. 3. The filled circles appearing in the figure correspond to the 57 transition arrays generated by the configurations listed above. They are of the types  $4f^2nl$ - $4f^2n'l'$ ,  $4fnln'l'$ - $4fnln''l''$ , and  $nln'l'n''l'''$ - $n'l'n''l'''n''l''''$ , where  $nl$ ,  $n'l'$ ,  $n''l''$ , and  $n''l''''$  are different from the  $4f$  orbital. This procedure was already

used with success in the cases of Er III [8], Tm III [9], Ce II [10], and Yb IV [11]. This correction, although empirical, does provide a better agreement of theory with experiment for the lifetimes and, consequently for the derived oscillator strengths, particularly for the transitions involving  $4f$ - $5d$  matrix elements, the effects on the other types of transitions being, in most cases, negligible.

#### IV. DISCUSSION

Transition probabilities or lifetimes in Pr III are very sparse, the only published work available for comparison being that of Palmeri *et al.* [7]. A comparison between the new experimental data and the theoretical values obtained in this work is presented in Table II. In the same table we also give the values of the theoretical lifetimes as obtained previously in Ref. [7]. In fact, the experimental results are very close to the HFR results, as obtained in the present work. The fact that the differences between experiment and the new HFR values are smaller than those obtained when comparing with the results obtained by Palmeri *et al.* [7] is due to the consideration of the core-penetration effects in a more realistic way in the present work. It appears that the mean ratio between experimental and theoretical lifetimes is now  $\tau_{\text{exp}}/\tau_{\text{theor}} = 1.04 \pm 0.11$  for seven levels (excluding the level at  $62\,535.6 \text{ cm}^{-1}$  for which the discrepancy is somewhat larger), the experimental lifetimes being in most cases, in agreement with the theoretical ones within the quoted uncertainties. It also appears that some levels, and particularly the level at  $62\,535.6 \text{ cm}^{-1}$ , are extremely sensitive to a correct consideration of the penetration contribution in the calculation of the line strengths.

Using the laser-induced fluorescence lifetimes obtained in the present work and theoretical branching fractions deduced



within the framework of the new HFR calculation, it was possible to derive a new set of normalized oscillator strengths and transition probabilities for the lines depopulating the levels for which lifetimes have been measured. The corresponding results are reported in Table III, where only the most intense transitions ( $gA > 10^8 \text{ s}^{-1}$ ) are quoted. More detailed results will be available in the DREAM database at the address <http://www.umh.ac.be/~astro/dream.shtml>.

## ACKNOWLEDGMENTS

This work was financially supported by the Swedish Natural Science Research Council (NRF), by the National Natural Science Foundation of China, by the Belgian National Fund for Scientific Research, and also by the European Community Access to Large-Scale Facilities program (Contract No. ERBFMGECT 950020).

- 
- [1] W. P. Bidelman, in *Abundance Determination in Stellar Spectra*, edited by H. Hubenet, IAU Symposium No. 26 (Academic, London, 1966), p. 229.
- [2] G. C. L. Aikman, C. R. Cowley, and H. M. Crosswhite, *Astrophys. J.* **232**, 812 (1979).
- [3] G. Mathys and C. R. Cowley, *Astron. Astrophys.* **253**, 199 (1992).
- [4] T. Ryabchikova, N. Piskunov, I. Savanov, F. Kupka, and V. Malanushenko, *Astron. Astrophys.* **343**, 229 (1999).
- [5] D. S. Leckrone, S. G. Johansson, and G. M. Wahlgren, in *The Scientific Impact of the Goddard High Resolution Spectrograph*, edited by J. C. Brandt, T. B. Ake III, and C. C. Petersen, ASP Conference Series Vol. 143 (Publishers City, 1998), p. 135.
- [6] C. R. Cowley, W. P. Bidelman, and G. Mathys, *Bull. Am. Astron. Soc.* **30**, 1317 (1998).
- [7] P. Palmeri, P. Quinet, Y. Frémat, J.-F. Wyart, and E. Biémont, *Astrophys. J. Suppl.* **129**, 367 (2000).
- [8] E. Biémont, H.-P. Garnir, T. Bastin, P. Palmeri, P. Quinet, Z. S. Li, Z. G. Zhang, V. Lokhnygin, and S. Svanberg, *Mon. Not. R. Astron. Soc.* **321**, 481 (2001).
- [9] Z. S. Li, Z. G. Zhang, L. Lokhnygin, S. Svanberg, T. Bastin, E. Biémont, H.-P. Garnir, P. Palmeri, and P. Quinet (unpublished).
- [10] Z. G. Zhang, S. Svanberg, Zhankui Jiang, P. Palmeri, P. Quinet, and E. Biémont, *Phys. Scr.* **63**, 122 (2001).
- [11] J.-F. Wyart, W.-U. L. Tchang-Brillet, N. Spector, P. Palmeri, P. Quinet, and E. Biémont, *Phys. Scr.* **63**, 113 (2001).
- [12] S. Svanberg, J. Larsson, A. Persson, and C.-G. Wahlström, *Phys. Scr.* **49**, 187 (1994).
- [13] W. C. Martin, R. Zalubas, and L. Hagan, *Atomic Energy Levels—The Rare-Earth Elements*, National Standard Reference Data Series-National Bureau of Standards, Washington, D.C. (U.S. GPO, Washington, DC, 1978), Vol. 60.
- [14] J. Sugar, *J. Opt. Soc. Am.* **53**, 831 (1963).
- [15] J. Sugar, *J. Res. Natl. Bur. Stand., Sect. A* **73**, 333 (1969).
- [16] H. Crosswhite, H. M. Crosswhite, and B. R. Judd, *Phys. Rev.* **174**, 89 (1968).
- [17] J. Sugar, *J. Res. Natl. Bur. Stand., Sect. A* **78**, 555 (1974).
- [18] J.-F. Wyart, J. Blaise, and P. Camus, *Phys. Scr.* **9**, 325 (1974).
- [19] J.-F. Wyart and P. Palmeri (unpublished).
- [20] Z. S. Li, J. Norin, A. Persson, C.-G. Wahlström, S. Svanberg, P. S. Doidge, and E. Biémont, *Phys. Rev. A* **60**, 198 (1999).
- [21] Z. S. Li *et al.* (unpublished).
- [22] J. Migdalek and W. E. Baylis, *J. Phys. B* **11**, L497 (1978).
- [23] R. D. Cowan, *The Theory of Atomic Structure and Spectra* (University of California Press, Berkeley, 1981).
- [24] S. Fraga, J. Karwowski, and K. M. S. Saxena, *Handbook of Atomic Data* (Elsevier, Amsterdam, 1976).